

Dynamics of superradiant media in a resonator

A.M. Basharov, G.G. Grigoryan, N.V. Znamenskii, Yu.V. Orlov, A.Yu. Shashkov, T.G. Yukina

Abstract. Experimental results and a theoretical model describing superradiance of praseodymium ions in the trifluoro lanthanum matrix at the ${}^3P_0 - {}^3H_6$ transition upon coherent excitation of the adjacent ${}^3H_4 - {}^3P_0$ transition are presented. It is found that when a superradiant medium is placed into a resonator, whose eigenfrequency is close to the superradiant transition (${}^3P_0 - {}^3H_6$) frequency, the superradiant pulse duration decreases and its modulation appears, which is independent of the resonator length. It is shown that these properties are qualitatively described within the framework of the mean-field model of coherent radiation of superradiant media in a resonator.

Keywords: superradiance, coherent excitation, three-level system, mean field model, resonator, modulation, spike structure.

1. Introduction

Optical effects appearing upon coherent excitation of praseodymium ions in the matrix of trifluoro lanthanum $\text{LaF}_3:\text{Pr}^{3+}$ still attract the attention of researchers. Coherent radiation in the $\text{LaF}_3:\text{Pr}^{3+}$ crystal at the ${}^3P_0 - {}^3H_6$ transition of the praseodymium ion excited at the adjacent ${}^3H_4 - {}^3P_0$ transition by a nanosecond laser pulse was studied in papers [1–7]. Apart from the fact that this coherent radiation well demonstrates the superradiance process, it impedes the observation of the photon echo resonant with the ${}^3H_4 - {}^3P_0$ transition upon interaction of two exciting radiation pulses. Obviously, this superradiance is inherent in all the optical phenomena related to the excitation of the ${}^3H_4 - {}^3P_0$ transition of the praseodymium ion. In this connection, a thorough study of this superradiance under different condition is quite urgent.

In this paper, we found and studied new properties of superradiance at the ${}^3P_0 - {}^3H_6$ transition of the praseodymium ion. Unlike papers [6, 7], which considered single-pulse nonresonator superradiance, we studied the multipulse regime. It was found that the spike structure of superradiance changes when the superradiant medium is placed into a resonator: spikes become smoothed, the better the

longer the resonator, while the total duration of the radiation pulse decreases. In this case, the superradiance intensity modulation appears at the frequency that is independent of the resonator length. The latter was surprising because we expected that superradiance would be modulated at the frequency related to the difference between the superradiant transition frequency and the resonator eigenfrequency. It turned out, however, that all these properties are qualitatively described within the framework of the mean superradiance field model being developed in this paper for the case of different superradiance channels.

To analyse superradiance of praseodymium ions in the trifluoro lanthanum matrix, we proposed the model of a three-level medium [5], whose distinctive feature involves describing the superradiant transition within the framework of the mean field model of a microresonator when the medium is optically thick and the description of the medium at the exciting transition frequency corresponded to the case of an optically thin medium. It is shown in this paper how this model can be naturally supplemented by taking into account the resonator channel of superradiance, the terms, which correspond to the nonresonator and resonator channels, entering symmetrically into the theoretical equations. The simplest analysis of basic theoretical equations shows that an increase in the number of superradiance channels leads to a decrease both in the duration of a separate superradiance spike and the time of energy extraction from the medium. In this case, the decrease in the total superradiance pulse duration is simply explained: the rate of energy extraction from the medium increases with the number of channels, while the superradiant pulse duration decreases. The modulation of the superradiance intensity seemingly could be also easily explained by the beats of radiation frequencies in different channels, which are characterised by different carrier frequencies. However, the numerical analysis of the model being developed indicates that the modulation frequency (in a certain region of parameters) is independent of the carrier frequencies of superradiance channels. In our experiment, different resonator lengths correspond to different frequencies of the superradiance channels, and the independence of the modulation frequency of the frequencies of superradiance channels is confirmed by the discovered effect of the independence of the modulation frequency of the resonator superradiance intensity of the resonator length.

A.M. Basharov, G.G. Grigoryan, N.V. Znamenskii, Yu.V. Orlov, A.Yu. Shashkov, T.G. Yukina ‘Kurchatov Institute’ Russian Research Centre, pl. Akad. Kurchatova 1, 123182 Moscow, Russia; e-mail: basharov@gmail.com, shash@issph.kiae.ru

Received 22 November 2007; revision received 10 November 2008
Kvantovaya Elektronika 39(3) 251–255 (2009)
Translated by I.A. Ulitkin

2. Experiment

The sample of the $\text{LaF}_3:\text{Pr}^{3+}$ crystal doped with praseodymium ions (the atomic concentration was 0.5%) was

placed in a helium optical cryostat with fused quartz windows. The cryostat temperature could be varied in the range from 4.2 K to room temperature. An organic dye laser beam was focused into the crystal with the help of a long-focus lens (with the focal distance of 100 cm) into a spot of size 0.5×0.5 mm. The angle of incidence was $\sim 2^\circ$ with respect to the normal to the crystal face. The laser linewidth $\Delta\omega_p/(2\pi c)$ did not exceed 0.09 cm^{-1} . The laser pulse was bell-shaped with the duration at the basis $\tau_p = 15$ ns, which is significantly shorter than the longitudinal ($1/\gamma_2$) and transverse ($1/\gamma_{21}$) relaxation times of the ${}^3\text{H}_4 - {}^3\text{P}_0$ transition at liquid helium temperatures, which are 47 and 2.4 μs , respectively. The radiation frequency ω_p of the dye laser was tuned within the inhomogeneous emission linewidth of the ${}^3\text{H}_4 - {}^3\text{P}_0$ transition of the praseodymium ion centred at $\omega_1/(2\pi c) = 20930.1 \text{ cm}^{-1}$.

The pump radiation intensity I_p at the crystal input was determined by the radiation resistance of the latter and could achieve $\sim 40 \text{ MW cm}^{-2}$. Radiations under study were recorded with a streak camera.

For the intensity $I_p \approx 20 \text{ W cm}^{-2}$ (and higher) at the output from the crystal we observed superradiance at the frequency $\omega/(2\pi c) = 16708.6 \pm 0.1 \text{ cm}^{-1}$ of the ${}^3\text{P}_0 - {}^3\text{H}_6$ transition. It was excited both in the forward and backward direction and had the spectral width $\Delta\omega/(2\pi c) \approx 0.04 \text{ cm}^{-1}$. Superradiance was generated by tuning the frequency ω_p within the band of width 0.53 cm^{-1} , which is approximately 5–7 times smaller than the inhomogeneous width of the ${}^3\text{H}_4 - {}^3\text{P}_0$ transition. Superradiance was observed in the temperature range from 4.2 to 25 K. Its beam had a divergence of ~ 40 mrad and the angle between the forward and backward beams was $\sim 2^\circ$. The propagation directions of these beams were close to the normals to the opposite faces of the crystal.

Chronograms obtained with the help of the streak camera showed that superradiance consists of a high-power pulse ($\tau = 10 - 15$ ns) studied by us in [3], and a weaker ‘tail’ of a train of spikes with a decreasing intensity, which are random in duration (5–50 ns) and repetition period (Fig. 1). The total emission duration achieves 2 μs at 4.5 K and decreases with increasing temperature. At temperatures above 25 K superradiance disappears.

When an optical resonator was placed outside the cryostat, apart from nonresonator superradiance in the two close directions, there appeared radiation with the divergence of ~ 6 mrad, which was caused by the resonator. Both resonator mirrors had the reflectivity of $\sim 65\%$ and the resonator length was 45, 90 or 135 cm. Typical chronograms of resonator generation are shown in Fig. 2. It

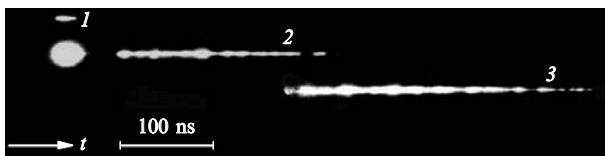


Figure 1. Chronograms of the pump pulse and superradiance pulse in the absence of the resonator: a short track of the pump pulse in the sample (1), a track of stochastic superradiance spikes after the streak camera start-up with the pump pulse advance (the first spike is more intense than other spikes, therefore it is overexposed) (2) and a track of stochastic superradiance spikes after the streak camera start-up with a delay of 300 ns (3). The crystal temperature is 5 K.

appears with a delay of ~ 20 ns and more relative to the exciting pulse. One can see that the total duration of lasing decreases down to 1 μs . At the resonator length 45 cm, the duration of random spikes and their repetition period increase up to 100 ns and more, spikes becoming smooth. Random spikes disappear with further increasing the resonator length. The lasing intensity increases rather monotonically and then falls. In addition, at all lengths of the resonator the intensity proves regularly modulated with the characteristic time 5–10 ns. We observed no dependence of this time on the resonator length.

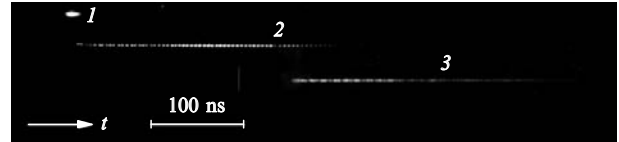


Figure 2. Chronograms of the pump pulse and superradiance pulse in the presence of a 90-cm-long resonator: a short track of the pump pulse in the sample (1), a track of stochastic superradiance spikes after the streak camera start-up with the pump pulse advance (2) and a track of stochastic superradiance spikes after the streak camera start-up with a delay of 300 ns (3). One can see regular radiation modulation. The crystal temperature is 5 K.

3. Model and basic equations

In the simplest case, the generation of superradiance can be represented as follows. The levels of the praseodymium ion in the spectral region of interest form a three-level system with a Λ configuration, which at the frequency of the optically allowed transition from the ground $E_1 \rightarrow E_3$ state is excited by the external coherent field, while at the transition from the excited level to the metastable $E_3 \rightarrow E_2$ level superradiance is emitted. In this case, the medium is optically thin at the frequency of the $E_1 \rightarrow E_3$ transition, while it is optically thick at the frequency of the $E_3 \rightarrow E_2$ transition (Fig. 3).

The system of equations describing this medium in the case of its excitation by coherent pulses and of emission of superradiant pulses and photon echo was derived and analysed in detail from the point of view of transformation of coherence during superradiance in papers [8, 9]. How-

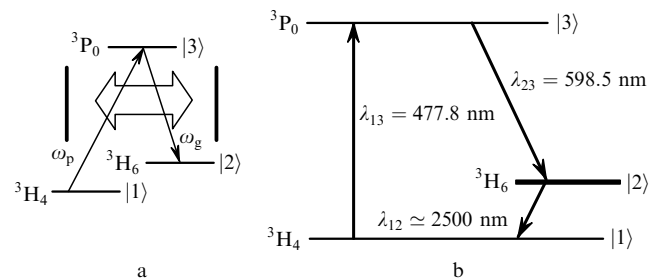


Figure 3. Three-level system with Λ configuration in which the transition from the ground state E_1 is in resonance with the external pump wave with the frequency ω_p and the frequency of the adjacent $E_3 \rightarrow E_2$ transition coincides with the frequency ω_g of the low- Q resonator (a) and the energy level diagram of the praseodymium ion in the frequency region under study (b).

ever, to describe the superradiance properties mentioned in Introduction and section 2, which are caused by placing a superradiant medium in the resonator, we can restrict ourselves by the following simplification. Because superradiance is emitted with some time delay with respect to the exciting pulse, we will consider the excitation (population) of the upper E_3 level by a short high-power pulse of coherent radiation, which is resonant to the $E_1 \rightarrow E_3$ transition, separately from the process of superradiance emission at the frequency of the $E_3 \rightarrow E_2$ transition. Then, the population process of the E_3 level will be described by ordinary Bloch equations for a two-dimensional medium. Their general solution can be found, for example in Chapter 2 of monograph [10]. After the upper E_3 level is populated, there occurs the stage of its superradiant decay with a transition to the metastable E_2 level. This stage is well studied (see monographs [11, 12]) and is described rather accurately by the system of Maxwell–Bloch equation in the mean field approximation $\bar{\mathcal{E}}$ [13, 14], which has the form:

$$\begin{aligned} \frac{d\bar{\mathcal{E}}}{dt} + \sigma\bar{\mathcal{E}}(t) &= i s_0 \bar{R}_{32}, & \frac{d\bar{R}_{32}}{dt} &= i\Delta\omega_2 \bar{R}_{32} + i\bar{n}_2 \frac{d_{32}\bar{\mathcal{E}}}{\hbar}, \\ \frac{d\bar{n}_2}{dt} &= 4\text{Im}\left(\bar{R}_{32}^* \frac{d_{32}\bar{\mathcal{E}}}{\hbar}\right), \end{aligned} \quad (1)$$

where the bar means averaging over the crystal length, in this case $\bar{R}_{32}^* \bar{\mathcal{E}} \approx \bar{R}_{32}^* \bar{\mathcal{E}}$, etc. [13, 14]; d_{32} is a matrix element of the dipole moment operator of the $E_3 \rightarrow E_2$ transition; σ^{-1} is the lifetime of a superradiance photon in the crystal; $s_0 = 2\pi\omega N d_{32}^*$; N is the density of praseodymium ions. In equations (1), the detuning $\Delta\omega_2 = \omega - \omega_2$ from the central frequency $\omega_2 = (E_3 - E_2)/\hbar$ of the $E_3 \rightarrow E_2$ transition is preserved so that it be convenient to generalise them for the case when the resonator generation is taken into account. The expression for the electric field of superradiance with the frequency $\omega = kc$ can be represented in the form

$$\begin{aligned} E &= \mathcal{E} \exp(-i\omega t) + \text{c.c.}, \\ \mathcal{E} &= \mathcal{E}^{(+)} \exp(ikz) + \mathcal{E}^{(-)} \exp(-ikz), \\ \bar{\mathcal{E}} &= \frac{1}{L} \int_0^L dz \mathcal{E}^{(+)} \approx \frac{1}{L} \int_0^L dz \mathcal{E}^{(-)}, \end{aligned} \quad (2)$$

where L is the characteristic size of the crystal. Matrix elements ρ_{22} , ρ_{33} and ρ_{32} of the density matrix of praseodymium ions describe the $E_3 \rightarrow E_2$ transition and quantities \bar{R}_{32} and \bar{n}_2 by the relations

$$\begin{aligned} \rho_{32} &= R_{32} \exp(-i\omega t), & R_{32}^{(\pm)} &= \frac{k}{2\pi} \int_{-\pi/k}^{\pi/k} dz R_{32} \exp(\mp ikz), \\ \bar{R}_{32} &= \frac{1}{L} \int_0^L dz R_{32}^{(+)} \approx \frac{1}{L} \int_0^L dz R_{32}^{(-)}, \\ n_2 &= \rho_{22} - \rho_{33}, & \bar{n}_2 &= \frac{1}{L} \int_0^L dz n_2. \end{aligned} \quad (3)$$

Because the equations of the pulsed resonator generation (see, for example, [15]) can be reduced to Eqns (1), we will introduce the average amplitude $\bar{\mathcal{E}}_g$ of the resonator mode to describe the resonator channel of superradiance emission

with the frequency $\omega_g = k_g c$. We will denote the electric field strength for the resonator mode by E_g . In this case, similarly to expressions (2), we have

$$\begin{aligned} E_g &= \mathcal{E}_g \exp(-i\omega_g t) + \text{c.c.}, \\ \mathcal{E}_g &= \mathcal{E}_g^{(+)} \exp(ik_g z) + \mathcal{E}_g^{(-)} \exp(-ik_g z), \\ \bar{\mathcal{E}}_g &= \frac{1}{L} \int_0^L dz \mathcal{E}_g^{(+)} \approx \frac{1}{L} \int_0^L dz \mathcal{E}_g^{(-)}. \end{aligned} \quad (4)$$

To take the resonator generation channels into account, equations (1) can be ‘corrected’ as follows:

$$\begin{aligned} \frac{d\bar{\mathcal{E}}}{dt} + \sigma\bar{\mathcal{E}}(t) &= i s_0 \bar{R}_{32} \exp(i\delta t), & \frac{d\bar{\mathcal{E}}_g}{dt} + \sigma_g \bar{\mathcal{E}}_g(t) &= i s_0 \bar{R}_{32}, \\ \frac{d\bar{R}_{32}}{dt} &= i\Delta\omega_2 \bar{R}_{32} + i\bar{n}_2 \frac{d_{32}[\bar{\mathcal{E}}_g + \bar{\mathcal{E}} \exp(-i\delta t)]}{\hbar}, \\ \frac{d\bar{n}_2}{dt} &= 4\text{Im}\left(\bar{R}_{32}^* \frac{d_{32}[\bar{\mathcal{E}}_g + \bar{\mathcal{E}} \exp(-i\delta t)]}{\hbar}\right), \end{aligned} \quad (5)$$

where $\delta = \omega - \omega_g$ is the difference between the frequencies of nonresonator and resonator generation and σ_g is the velocity of photon emission from the crystal in the resonator generation channel.

It is convenient to represent Eqns (5), which describe superradiance under conditions of existence of several channels of superradiance emission, in the generalised form:

$$\begin{aligned} \frac{d\mathcal{E}_n}{dt} + (\sigma_n + i\delta_n)\mathcal{E}_n &= i s_0 R_{32}, & \frac{dR_{32}}{dt} &= i n_2 d_{32} \hbar^{-1} \sum_n \mathcal{E}_n, \\ \frac{dn_2}{dt} &= 4\text{Im}\left(R_{32}^* d_{32} \hbar^{-1} \sum_n \mathcal{E}_n\right), \end{aligned} \quad (6)$$

where n is the channel number ($n = 1, \dots, N_c$) of energy extraction due to coherent radiation with the carrier frequencies close to the frequencies of the $E_3 \rightarrow E_2$ transition. We omitted the averaging signs and slightly changed the definitions of the basic quantities in selecting the phase fast-oscillating factor. Now the matrix elements of the complete density matrix and the electric field strength in the n th channel are described by the expressions $\rho_{32} = R_{32} \exp(-i\omega_2 t)$ and $E_n = \mathcal{E}_n \exp(-i\omega_2 t) + \text{c.c.}$, the difference $\omega_2 - \delta_n$ representing a carrier radiation frequency in the n th channel. Terms describing the resonator and non-resonator radiation channels enter symmetrically into Eqns (6).

4. Superradiance in a resonator

Let the lower level of the three-level system be populated at the initial instant of time and the pump pulse, which is resonant to the $E_1 \rightarrow E_3$ transition, be ultrashort with the amplitude A_p and the area

$$\theta = 2|d_{31}| \hbar^{-1} \int A_p dt,$$

where d_{31} is the matrix element of the dipole moment operator for the $E_1 \rightarrow E_3$ transition.

Note that the pump pulse duration τ_p is lower not only than the characteristic relation times in the medium but also than the times of the instability development in the T_{unst} system. The action of this θ pulse produces inversion population at the $E_3 \rightarrow E_2$ transition, which affects the initial conditions for Eqns (6)

$$R_{32} = 0, \quad n_2 = -\sin^2(\theta/2), \quad \mathcal{E}_n = 0. \quad (7)$$

For $\theta = \pi$, the pulse transfers all the atoms to the upper excited level without any polarisation of the medium. At other values of θ the medium is simultaneously inverted and polarised.

Initial conditions (7) are also a solution of equations (6); however, this solution is unstable, i.e. the corresponding growth increments [responsible for the exponential ($e^{\lambda t}$) increase in small perturbations] are determined by the expression (for $\delta_n = 0$ and $\sigma_1 = \sigma_2 = \sigma$, $N_c = 2$)

$$\lambda = -\frac{\sigma}{2} \pm \left[\frac{\sigma^2}{4} + 2 \frac{d_{32}}{\hbar} s_0 \sin^2(\theta/2) \right]^{1/2}.$$

The instability rise time

$$T_{\text{unst}} \sim \hbar \frac{[\sigma^2 + 4\pi\omega N |d_{32}|^2 \hbar^{-1} \sin^2(\theta/2)]^{1/2} + \sigma}{4\pi\omega N |d_{32}|^2 \sin^2(\theta/2)} \quad (8)$$

with respect to the order of the quantity corresponds to the time delay of the superradiance pulse in two-level systems [11, 12] at small σ . In the simplest case, Eqns (6) can be reduced (see below) to Eqns (1) responsible for the development of instabilities and describing superradiance, the method for their analysis and solution being presented in Chapter 1 of monograph [12].

First of all, we will discuss the effect of the decrease in the coherent radiation duration when the medium is placed in the resonator. This effect is completely caused by the increase in the number of channels of energy extraction from the crystal. In the simplest way it can be described in the particular case

$$\begin{aligned} \sigma_1 = \sigma_2 = \dots = \sigma, \quad \delta_1 = \delta_2 = \dots = \delta, \\ \mathcal{E}_1 = \mathcal{E}_2 = \dots = \mathcal{E}, \quad \sum_n \mathcal{E}_n = N_c \mathcal{E}. \end{aligned} \quad (9)$$

After introducing the notation

$$\sqrt{N_c} \mathcal{E} = \mathcal{E}', \quad t \sqrt{N_c} = t', \quad \sigma / \sqrt{N_c} = \sigma', \quad \delta / \sqrt{N_c} = \delta' \quad (10)$$

equations (6) take the form

$$\begin{aligned} \frac{d\mathcal{E}'}{dt'} + (\sigma' + i\delta')\mathcal{E}' = is_0\rho_{32}, \quad \frac{d\rho_{32}}{dt'} = in_2 d_{32} \hbar^{-1} \mathcal{E}', \\ \frac{dn_2}{dt'} = 4\text{Im}(\rho_{32}^* d_{32} \hbar^{-1} \mathcal{E}') \end{aligned} \quad (11)$$

and under assumptions made, they coincide with equations (1) describing nonresonator generation [11, 12]. It immediately follows that in the presence of the resonator the characteristic duration of coherent radiation pulse decreases and the rate of energy extraction from the system increases. This corresponds to the experimentally observed change in the duration of the coherent radiation pulse in non-resonator and resonator regimes.

Recall that Eqns (1) of the semiclassical superradiance model can be reduced to the motion equation of a nonlinear pendulum with friction [11, 12]. In the case of low friction and the initial condition corresponding to the unstable equilibrium position, we obtain solutions expressed through the elliptic Jacobi functions [5, 12]. They are very sensitive to initial fluctuations but after the pendulum leaves the unstable state, they demonstrate only a decaying regular periodic dynamics. These solutions describe the oscillatory regime of superradiance. In the case of strong friction, the solutions for the predamped nonlinear pendulum are reduced to a hyperbolic secant, whose shape is insensitive to small fluctuations of initial conditions and corresponds to the single-pulse regime of superradiance [11, 12].

In the case of a low- Q resonator,

$$\sigma \gg |d_{32}|/\hbar, \quad \sigma \gg T_{\text{rel}} \quad (12)$$

(T_{rel} is the characteristic relaxation time of a three-level system), the single-pulse regime of superradiance is realised [11, 12]. In this case, at $\delta = 0$ the solution of Eqns (6) has a classical form of a hyperbolic secant [12, 15] and for the variables of one channel is written in the form

$$\mathcal{E} = -s_0 \sigma^{-1} \frac{\sin^2(\theta/2)}{2 \cosh[A t N_c \sin^2(\theta/2)]},$$

$$A = d_{32} s_0 \sigma^{-1} \hbar^{-1} = 2\pi\omega N |d_{32}|^2 \sigma^{-1} \hbar^{-1}.$$

This solution also indicates that the single-pulse duration decreases with increasing the number of channels of energy extraction. Note that the described picture corresponds to the simple assumptions about the energy balance in the case under study. Namely, an increase in the number of channels of energy extraction from the crystal, when the rate of energy extraction in each channel is constant, inevitably leads to a decrease in the duration of coherent radiation removing this energy.

If the carrier frequencies of radiation channels are different ($\delta_1 \neq \delta_2$), the equations should be analysed using numerical methods. In the case of two channels with $\delta_1 = -\delta_2 = \delta$ the time dependence of the radiation intensity in one of the channels in the single-pulse regime is presented in Fig. 4. One can see that adding a channel for energy extraction leads to radiation modulation, the modulation frequency in the range under study being independent of the frequency difference in the channels. An impression is formed that radiation is 'pumped' over from one channel to another but because the radiation pulse duration is determined by other parameters, the frequency of this 'pumping' is strictly specified by the laser pulse duration, and, hence, only the modulation depth depends on the frequency difference of radiation extraction channels.

It is obvious that the decrease in the spike duration in the single-pulse regime and the described modulation in the multipulse regime are a manifestation of the same effect consisting in a simple increase in the number of slightly different but essentially similar energy emission channels.

In the theory being developed, we do not discuss the relation between the obtained regularities and the peculiarities of the regular chaotic dynamics. The peculiarities of the nonresonator generation caused by the regular chaotic dynamics were discussed in our previous papers [5, 16]. It is obvious that the regularities found in them, which are

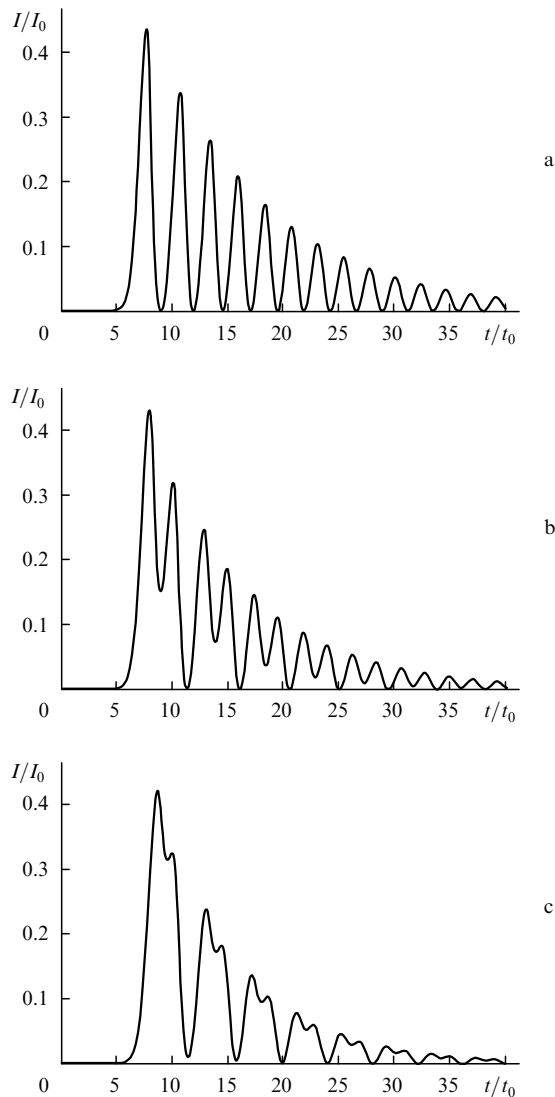


Figure 4. Time dependences of the coherent radiation intensity in the nonresonator (a) and resonator (b, c) regimes at $\sigma = 0.1/t_0$, $\theta = \pi$, $\delta = 0$ (a), $\delta = 0.4/t_0$ (b) and $0.7/t_0$ (c); $I_0 = \hbar\omega Nc$, $t_0 = [\hbar/(2\pi\omega N|d_{32}|^2)]^{1/2}$. Thermal fluctuations of the initial polarisation of the medium are equal to 0.0001.

caused by the peculiarities of the deterministic chaos, can be observed in a certain region in the case considered in this paper.

5. Conclusions

To simplify the theory, we have used the model of a three-level medium with a different optical density at different resonance frequencies by neglecting the Lorentzian field. This has allowed us to describe the process of superradiance by a two-level model and to analyse, using this model, the experimental results in the simplest way and in some cases analytically. In the absence of mentioned simplifications, the reduced analysis of the problem is, obviously, possible only by using numerical methods. Taking into account the generality of the description of coherent processes in optically dense media [5], the results of numerical studies of coherent effects in three-level systems in other models [17–21] can be used to understand the role of different parameters and their influence on the described effects. In

addition, these results [17–21] can help evaluate the role of Lorentzian field.

Acknowledgements. This work was supported by the Russian Foundation for Basic Research (Grant No. 06-02-16147-a).

References

1. Kichinski R., Hartman S.R. *AIP Conf. Proc.*, **146**, 417 (1986).
2. Manykin E.A., Znamenskiy N.V., Marchenko D.V., Petrenko E.A. *Pis'ma Zh. Eksp. Teor. Fiz.*, **54**, 172 (1991).
3. Agafonov A.I., Grigoryan G.G., Znamenskiy N.V., Manykin E.A., Orlov Yu.V., Petrenko E.A. *Kvantovaya Elektron.*, **34**, 823 (2004) [*Quantum Electron.*, **34**, 823 (2004)].
4. Grigoryan G.G., Orlov Yu.V., Petrenko E.A., Shashkov A.Yu., Znamenskiy N.V. *Laser Phys.*, **15**, 602 (2005).
5. Basharov A.M., Grigoryan G.G., Znamenskiy N.V., Manykin E.A., Orlov Yu.V., Shashkov A.Yu., Yukina T.G. *Zh. Eksp. Teor. Fiz.*, **129**, 239 (2006).
6. Zuikov V.A., Kalachev A.A., Samartsev V.V., Shegeda A.M. *Laser Phys.*, **9**, 951 (1999).
7. Zuikov V.A., Kalachev A.A., Samartsev V.V., Shegeda A.M. *Laser Phys.*, **10**, 364 (2000).
8. Basharov A.M., Znamenskiy N.V. *J. Phys. B: At. Mol. Opt. Phys.*, **39**, 4443 (2006).
9. Basharov A.M. *Opt. Spektrosk.*, **101**, 448 (2006).
10. Maimistov A.I., Basharov A.M. *Nonlinear Optical Waves* (Dordrecht: Kluwer Acad. Press, 1999).
11. Andreev A.V., Emel'nov V.I., Il'inskiy Yu.A. *Kooperativnyye yavleniya v optike* (Cooperative Phenomena in Optics) (Moscow: Nauka, 1988).
12. Benedict M.G., Ermolaev A.M., Malyshev V.A., et al. *Super-Radiance: Multiatomic Coherent Emission* (Bristol, Philadelphia: IOP, 1996).
13. Bonifacio R., Lugiato L.A. *Phys. Rev. A*, **18**, 1129 (1978).
14. Gronchi M., Benza V., Lugiato L.A., et al. *Phys. Rev. A*, **24**, 1419 (1981).
15. Belenov E.M., Oraevskii A.N., Shcheglov V.A. *Zh. Eksp. Teor. Fiz.*, **56**, 2143 (1969).
16. Basharov A.M., Znamenskiy N.V., Shashkov A.Yu. *Opt. Spektrosk.*, **104**, 288 (2008).
17. Zaitsev A.I., Malyshev V.A., Ryzhov I.V., Trifonov E.D. *Zh. Eksp. Teor. Fiz.*, **115**, 505 (1999).
18. Malyshev V.A., Carreno F., Anton M.A., et al. *J. Opt. B: Quantum Semiclassic. Opt.*, **5**, 313 (2003).
19. Elyutin S.O., Maimistov A.I. *Opt. Spektrosk.*, **90**, 849 (2001).
20. Malyshev V.A., Ryzhov I.V., Trifonov E.D., Zaitsev A.I. *Opt. Commun.*, **180**, 59 (2000).
21. Andreev A.V., Shitlin S.L. *Kvantovaya Elektron.*, **22**, 1203 (1995) [*Quantum Electron.*, **25**, 1166 (1995)].